Experiments of Tokamak Discharge and Simulation of Magnetic Field Configuration in Tokamak-Helical Hybrid Device TOKASTAR-2*)

Makoto HASEGAWA, Kozo YAMAZAKI, Hideki ARIMOTO, Tetsutarou OISHI, Reiya NISHIMURA and Tatsuo SHOJI

Department of Energy Engineering and Science, Graduate School of Engineering, Nagoya University, Furo-cho, Chikusa-ku, Nagoya 464-8093, Japan

(Received 9 December 2011 / Accepted 7 May 2012)

TOKASTAR-2 is a small tokamak-helical hybrid device which can generate tokamak and helical configurations independently. In tokamak discharge experiment, the conductive shell was installed to increase plasma current by controlling the displacement of ohmically heated (OH) plasma. The suppression of the vertical displacement was demonstrated, but the OH plasma was still located slightly above the mid plane. To compensate this displacement, the balance between up and down vertical field coil currents should be adjusted. In addition, the construction of additional helical field coils is planned to form closed vacuum magnetic surfaces. The magnetic field line tracing analysis was carried out to determine the detailed shape and location of additional helical field coils. From the simulation, it was clarified that the location of magnetic surfaces and the averaged value of rotational transform can be controlled by adjusting coil current ratios.

Keywords: tokamak-helical hybrid, tokamak discharge, fast camera, helical coil, vacuum magnetic surface

DOI: 10.1585/pfr.7.2402116

1. Introduction

Some tokamak-helical combined configurations have been proposed for a compact steady-state system having no plasma current disruptions. TOKASTAR configuration is one of compact tokamak-helical hybrid confinement systems and this configuration has several advantages [1]. An experimental device C-TOKASTAR (Compact Tokamak/Stellarator Hybrid) was constructed and the existence of the vacuum magnetic surface was confirmed experimentally [2]. Based on these researches, the investigation of the relationship among the plasma current, helical magnetic configurations and confinement properties is needed to understand this configuration clearly. For this purpose, a new small device named TOKASTAR-2 was designed and constructed.

To suppress plasma current disruptions, TOKASTAR-2 challenges to evaluate the helical field effect externally applied to tokamak plasmas. According to the previous experiment in the conventional tokamak-stellarator hybrid machine [3], the plasma becomes free from disruption when the rotational transform externally applied to the plasma is larger than 0.14. Another purpose is to generate a low-aspect-ratio current-free helical plasma, in which we can confirm the current effect on the helical plasma. The experimental plan of TOKASTAR-2 is shown in Fig. 1. At the beginning, (1) an ECR plasma was produced in a simple toroidal field using eight toroidal field (TF) coils (N_{TF} = 50 turn) and 2.45 GHz radio frequency (RF) wave. Next, (2A) tokamak discharge were performed using TF coils, three ohmic heating (OH) coils (N_{OH1} = 44 turn × 2 and N_{OH2} = 42 turn) and a pair of vertical field (VF) coils (N_{VF} = 100 turn). The experiment of (3A) outer helical field application on tokamak plasma will be carried out.

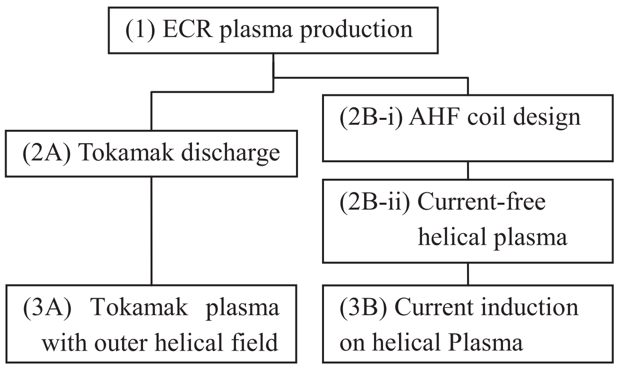

Fig. 1 TOKASTAR-2 experimental plans.

In addition, we analysed closed vacuum magnetic surfaces using magnetic field line tracing code and determined (2B-i) the detailed design of additional helical field (AHF) coil. The production of (2B-ii) current-free helical plasma is done experimentally using TF coils, a pair of helical field

author's e-mail: yamazaki@ees.nagoya-u.ac.jp
*) This article is based on the presentation at the 21st International Toki Conference (ITC21).

(HF) coils (N_{HF} = 98 turn) and two pairs of AHF coils. The (3B) plasma current induction on helical plasma will be done. In this paper, we focus on the experiments of (2A) and (2B-i).

2. OH Plasmas with the Conductive Shell

Using OH coils (pulsed power supply) and VF coils (static DC power supply), previously obtained plasma current is limited up to ~ 90A. Moreover, the vertical displacement of OH plasma was observed using a fast camera (40500 fps) [4]. Here, we installed a conductive shell to increase plasma current and to suppress the vertical plasma displacement. Figure 2 (a) shows one sector of the conductive shell. The total shell consists of four pieces and is installed inside the TF coils as shown in Fig. 2 (b).

Experimental conditions are as follows: The maximum TF coil current (I_{TF}) was set 110 A so that toroidal field of 0.0875 T is generated at R ~ 10 cm. The RF wave having the power of 0.6 kW was injected continuously. The loop voltage was about 4 V. The VF coil current (I_{VF}) was 6 A to generate static vertical field of 1.23×10^{-3} T. (In this experiment, optimal static vertical field was applied which had been surveyed previously to induce the largest plasma current.) Working gas was helium and its pressure was in the order of $10^{-3} \sim 10^{-2}$ Pa.

The fast camera was set on the mid plane of TOKASTAR-2. Figure 3 shows a plan view of the fast camera layout. Color images of an OH plasma are converted from monochromatic photographs as shown in Fig. 4. These images (a)~(f) were successive photographs taken by the fast camera (40500 fps) with the time interval of 24.7 µs. The helium gas pressure is 6.1×10^{-3} Pa. Plasma current measured by a Rogowski coil was about 320 A and this maximum value corresponds to the image (c). Comparing with previous case, the vertical displacement was suppressed and OH plasma located at Z ~ +2.3 cm. We will try to adjust up and down coil current of VF coils to locate the OH plasma near the mid plane.

Figure 5 shows the dependence of plasma current without and with the conductive shell on helium gas pressure. Compared with the values of plasma current without

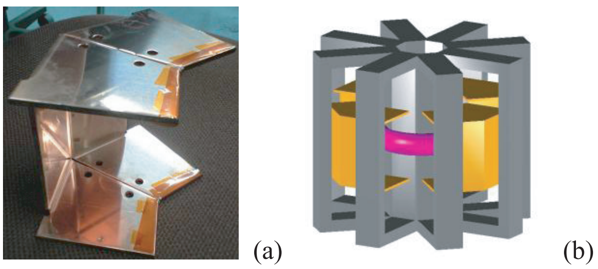

Fig. 2 Stabilizing conductive shell. Photo (a) shows one sector of the shell, and drawing (b) shows the layout of four sectors of the shell inside TF coils.

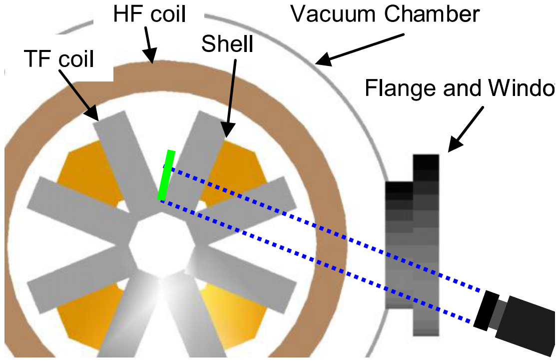

Fig. 3 Layout of fast camera (top view).

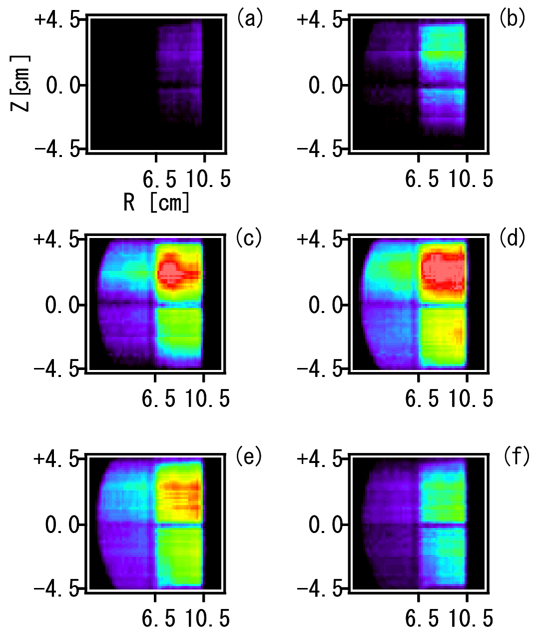

Fig. 4 Color images of OH plasma converted from successive monochromatic photograph taken by the fast camera. Time interval is 24.7 µs. The horizontal shadow line at Z = 0 cm is a Langmuir probe. The shadows at R < 6.5 cm and R > 10.5 cm denote the frame of TF coils.

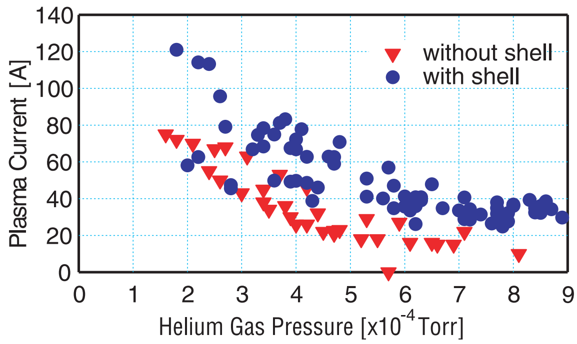

Fig. 5 Plasma current vs. helium gas pressure with or without the conductive shell. (1 Torr = 133 Pa).

the conductive shell, induced plasma current with the shell increases by 40 A. This increase in plasma current was due to the suppression of the vertical displacement by the conductive shell.

To induce more plasma current by applying appropriate time-varying vertical field, we are constructing a new pair of VF coil. New VF coils are installed inside the vacuum chamber and energized with pulsed power supply.

3. Magnetic Field Line Tracing Analysis of Helical Plasma

AHF coils are needed to generate the closed vacuum magnetic surface without plasma current. Within several engineering constraints, we defined the dimension of the AHF coil shown in Fig. 6 and evaluated the turn number of the coil using magnetic field line tracing analysis.

In the simulation, the configuration of each coil was reconstructed as single-filament current shown in Fig. 7. The TF, VF, HF and AHF coils are indicated black, red, yellow and green lines, respectively. From the arc of the HF coils, AHF coils are rotated by $\pi/8$ rad in toroidal direction. There is the vertical gap of 3 cm between HF coils and AHF coils, and this gap produces horizontal magnetic field which deforms magnetic surfaces to asymmetric ones. Each total current J is expressed as a product of the turn number N and the coil current I.

We evaluated the location of vacuum magnetic surface and the averaged value of rotational transform by changing coil current ratios which are normalized by J_{HF} ($= N_{HF}I_{HF}$). Figure 8 shows typical Poincaré plots of vacuum magnetic surface at each a quarter of toroidal period in a typical case of $J_{AHF}/J_{HF} = 1.20$, $J_{TF}/J_{HF} = 0.62$ and $J_{AHF}/J_{HF} = 0.09$.

Here, we kept $J_{TF}/J_{HF} = 0.62$ constant and varied other coil current ratios to understand the tendency of the location of magnetic surfaces. Figure 9 shows Poincaré plots of vacuum magnetic surface at $\phi = \pi/2$ rad within the TF coil frame. The ratio J_{AHF}/J_{HF} varies from 1.15 to 1.30. In Fig. 9, as additional helical field increases, magnetic surfaces are shifted vertically downward. The magnetic axis position can be set nearly on the mid plane at $J_{AHF}/J_{HF} = 1.25$, and the maximum plasma volume is obtained in the case of $J_{AHF}/J_{HF} = 1.20$.

Similarly, Fig. 10 shows Poincaré plots of vacuum

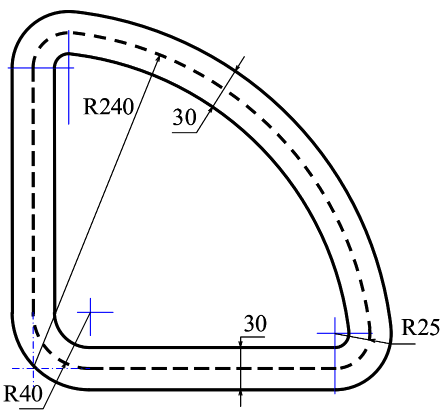

Fig. 6 Design of the AHF coil (mm).

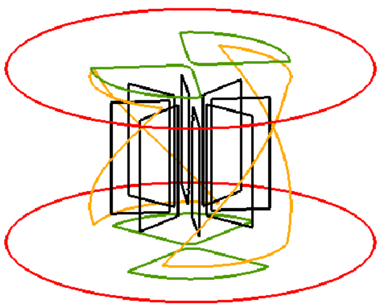

Fig. 7 Filament coil system used in the calculation.

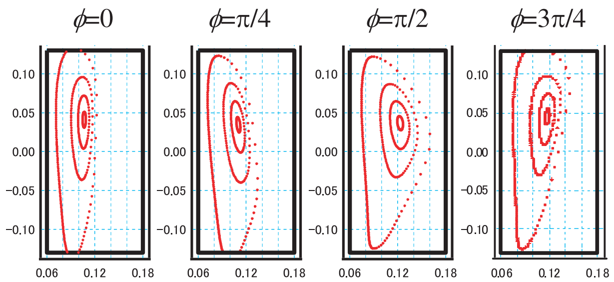

Fig. 8 Typical Poincaré plots of magnetic surfaces as a function of toroidal angle ϕ.

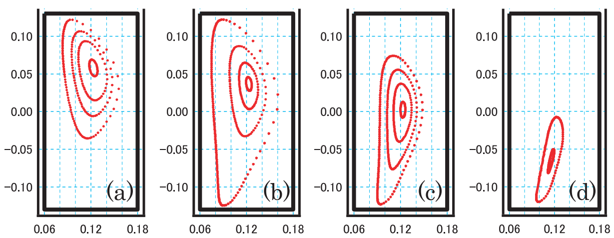

Fig. 9 Vertical shift of Poincarṕlots of magnetic surfaces at $\phi = \pi/2$ rad varying J_{AHF}/J_{HF} and keeping $J_{VF}/J_{HF} = 0.09$ and $J_{TF}/J_{HF} = 0.62$. Values of J_{AHF}/J_{HF} are (a) 1.15, (b) 1.20, (c) 1.25 and (d) 1.30.

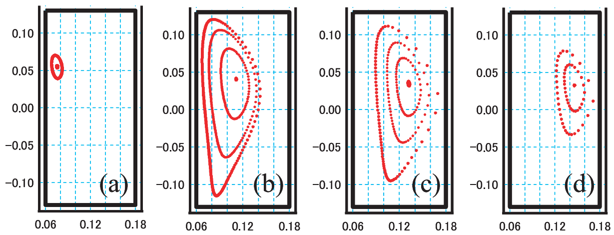

Fig. 10 Horizontal shift of Poincaré plots of magnetic surfaces at $\phi = \pi/2$ rad varying J_{VF}/J_{HF} and keeping $J_{AHF}/J_{HF} = 1.20$ and $J_{TF}/J_{HF} = 0.62$. Values of J_{VF}/J_{HF} are (a) 0.01, (b) 0.06, (c) 0.12 and (d) 0.18.

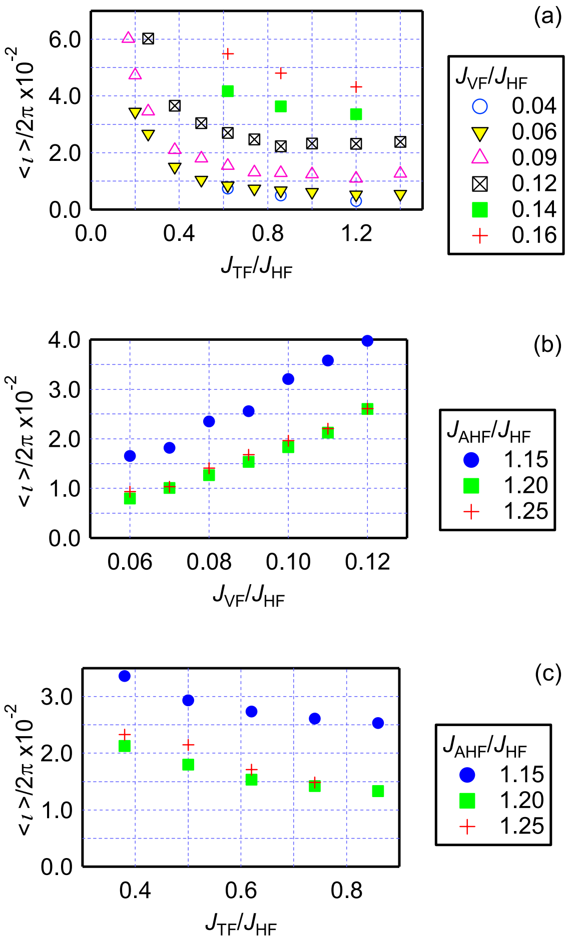

Fig. 11 Calculated average rotational transform of the last closed vacuum magnetic surface changing coil current ratios.

magnetic surface at $\phi = \pi/2$ rad varying the ratio J_{VF}/J_{HF}. When the vertical field increases, the magnetic surfaces shift horizontally in the outward direction.

The change in toroidal field and vertical field strengths also contributes to the change in averaged rotational transform. Figures 11 (a), (b) and (c) show averaged rotational transform ($\langle\iota\rangle/2\pi$) calculated using magnetic field line tracing code. Increasing J_{TF}/J_{HF} leads to the reduction of averaged rotational transform. On the contrary, the increase in J_{VF}/J_{HF} leads to the increase in averaged rotational transform. It was considered that the adjustment of these coil current ratios is important to control the location of magnetic surface and the value of rotational transform in the case that the external helical field is applied on the tokamak plasmas.

Since the number of pulsed power supply is limited, we plan to connect HF coils and AHF coils in series in the future helical plasma experiments. To keep the magnetic axis position on the mid plane, the optimal ratio N_{AHF}/N_{HF} is 1.25 as shown in Fig. 8. Moreover, this ratio should be increased in the case of irregular gap between HF coil and AHF coil, which was not shown in the present paper. The number of conductor layers (12 layers) in the coil cross-section was also evaluated to determine the AHF turn number. Finally we decided to construct AHF coils with N_{AHF} = 126 turn (N_{AHF}/N_{HF} = 1.28). Even in this final design, we can produce various configurations by driving unbalanced currents between upper and lower VF coils.

4. Summary

The conductive shell was installed in TOKASTAR-2 device. The vertical displacement of OH plasma was suppressed and the plasma current increased slightly in the case that a static vertical field is applied.

Magnetic field line tracing analysis was carried out to determine the detailed design of AHF coils. It is clarified by the simulation that controlling the magnetic surface position and the averaged rotational transform are possible by adjusting coil current ratios. Finally we determined the size (30 mm × 300 mm cross-section), the location ($\Delta\phi = \pi/8$) and the turn number (N_{AHF} = 126) of the AHF coil.

[1] K. Yamazaki and Y. Abe, Tokastar: Tokamak-Stellarator Hybrid with Possible Bean-Shaped operation, Research Report of the Institute of Plasma Physics, Nagoya, Japan, IPPJ-718 (1985).

[2] Y. Taira, K. Yamazaki, H. Arimoto and T. Shoji, Plasma Fusion Res. **5**, S1025 (2010).

[3] J. Fujita *et al.*, IEEE Trans. Plasma Sci. **PS-9**, 180 (1981).

[4] M. Hasegawa, K. Yamazaki, H. Arimoto, T. Oishi, K. Baba, M. Suwabe and T. Shoji, Plasma Fusion Res. **6**, 2402141 (2011).